

Electron-hole cotunneling effect in coupled single-electron transistors

Mincheol Shin*

School of Engineering, Information and Communications University, Daejeon 305-714, Republic of Korea

Gwang-Hee Kim

Department of Physics, Sejong University, Seoul 143-747, Republic of Korea

(Received 11 March 2002; published 16 December 2002)

We have found theoretically that parallel coupled single-electron transistors undergo a unique crossover from a cotunneling-only state to a predominantly sequential-tunneling state. As a result of the competition between the cotunneling and the sequential tunneling in the course of the crossover, a current dip instead of the usual current peak is observed.

DOI: 10.1103/PhysRevB.66.233308

PACS number(s): 73.23.Hk, 73.20.-r, 73.40.Gk

In parallel coupled one-dimensional (1D) arrays where each electrode of one of the arrays is capacitively coupled to electrodes in the other, the electron-hole transport gives rise to the so-called quantum current mirror effect, where identical currents of opposite signs flow in the two arrays.¹⁻³ The relevant transport mechanism is the simultaneous transfer of e - h pairs over the facing tunnel junctions, and the detection of the mirror current in the unbiased array directly proved the existence of such a macroscopic quantum tunneling process. On the other hand, there also exists a sequential tunneling of electrons and holes, which usually occurs at higher bias voltages. In this work, we have studied the crossover from the cotunneling-only state to the predominantly sequential-tunneling state in the parallel coupled 1D arrays, considering the simple case where each 1D array consists of two tunnel junctions with a separate gate attached to each middle island.^{4,5} The simple system we considered in this work enables us to investigate tunneling processes in the crossover regime in detail, and the appearance of the current dip is explained in the framework of the competition between the two tunneling mechanisms.

In Fig. 1, we show the parallel coupled single-electron transistors (SET's) where two single SET's are capacitively coupled via the capacitance C_α between the two metallic islands. Symmetric source-drain voltages V_1 and V_2 are applied separately to the lower and upper SET's, respectively. Separate gate voltages $V_{g,1}$ and $V_{g,2}$ are also applied to the lower and upper SET's, respectively. For simplicity, we assume that the four tunnel junctions in the system are identical with capacitance C and resistance R .

In Fig. 2(a), we show a typical stability diagram of a single SET with respect to the source-drain voltage V and the charge q induced by the gate. In the figure, Coulomb diamonds of $n=0$ and -1 , where n is the number of stationary electrons in the middle island, are shown. For the sweep over q at low bias voltages, there is a narrow region around $q=1/2$ where the crossover from the stable states $n=0$ to $n=-1$ takes place [Fig. 2(c)]. In the crossover region, both states $n=0$ and -1 are present and the tunneling processes $0 \rightarrow -1 \rightarrow 0$ take place, resulting in the nonzero current [Fig. 2(e)]. In comparison, a typical stability diagram of the parallel coupled SET's of Fig. 1 with respect to the gate-induced charges $q_1 (= C_g V_{g,1})$ and $q_2 (= C_g V_{g,2})$ is shown in Fig. 2(b). In the figure, the stable charge configuration of an in-

dividual hexagon is marked as (n_1, n_2) , where n_1 and n_2 are the number of electrons in islands 1 and 2, respectively. Analogously to the single SET case, there is a crossover from the stable states $(0, 0)$ to $(-1, 1)$ for the sweep along the line indicated in Fig. 2(b), where $q \equiv q_1 = -q_2$. Similarly to the single SET case, in the crossover region for the coupled SET's, both stable states $(0, 0)$ and $(-1, 1)$ are present, and the tunneling processes $(0,0) \rightarrow (-1,1) \rightarrow (0,0)$ take place. However, for some values of V_1 and V_2 , the crossover is not smooth: there are abrupt changes in the crossover region [see Fig. 2(d)] in contrast to the smooth transition for a single SET, and the current I_1 through the lower SET shows a dip around $q = \frac{1}{2}$ [Fig. 2(f)], which is the feature that does not exist in a single SET. The existence of the current dip in the coupled SET's, which is of purely quantum-mechanical origin, is the main result of this paper.

Let us first consider the energy and free energy of the coupled SET's. The potentials ϕ_1 and ϕ_2 of islands 1 and 2, respectively, are given by

$$\phi_1 = -\psi_0 \bar{n}_1 - \frac{\psi_1}{2} \bar{n}_2, \quad (1)$$

$$\phi_2 = -\psi_0 \bar{n}_2 - \frac{\psi_1}{2} \bar{n}_1, \quad (2)$$

where

$$\bar{n}_1 = n_1 - C_g V_{g,1}, \quad (3)$$

$$\bar{n}_2 = n_2 - C_g V_{g,2} \quad (4)$$

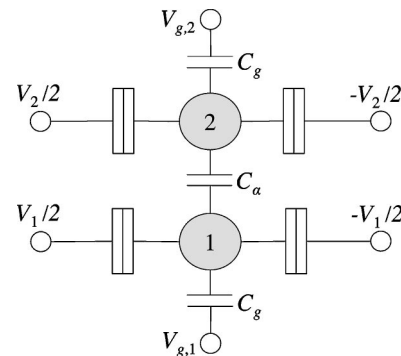


FIG. 1. The parallel coupled single-electron transistors. The lower and upper single-electron transistors, each having separate source, drain, and gate electrodes, are capacitively coupled via the capacitance C_α .

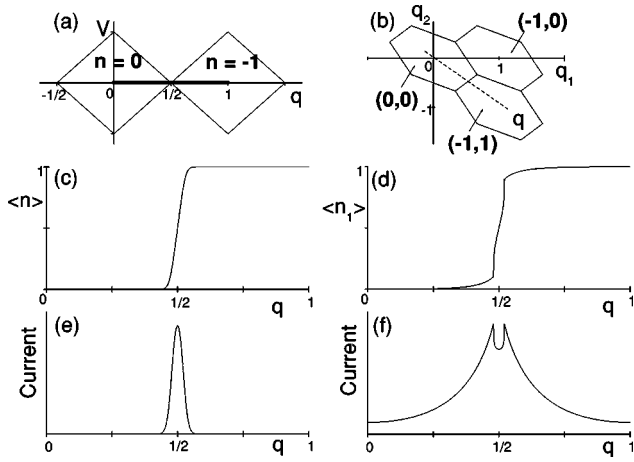


FIG. 2. Comparison of the stability diagram of (a) a single SET and (b) coupled SET's. Average charge on the middle island with respect to the gate sweep for (c) a single SET and (d) coupled SET's, and current with respect to the gate sweep for (e) a single SET and (f) coupled SET's. The thick line in (a) and the dashed line in (b) represent the paths along which the gate voltages are swept.

and

$$\psi_0 = \frac{1}{4} \frac{C_\alpha + 2}{C_\alpha + 1}, \quad (5)$$

$$\psi_1 = \frac{1}{2} \frac{C_\alpha}{C_\alpha + 1}. \quad (6)$$

n_1 and n_2 are the net charges on islands 1 and 2, respectively, and the capacitance and potential were scaled by the units $\tilde{C} = C + C_g/2$ and $\tilde{V} = e/\tilde{C}$, respectively. The electrostatic energy $E(n_1, n_2)$ for a charge configuration (n_1, n_2) is then

$$E(n_1, n_2) = \frac{1}{2} \psi_0 (\tilde{n}_1^2 + \tilde{n}_2^2) + \frac{1}{2} \psi_1 \tilde{n}_1 \tilde{n}_2, \quad (7)$$

where the first term represents the charging energy of the system and the second term the Coulomb energy for the charges (n_1, n_2) . The free energy of the system is then given by

$$F(n_1, n_2) = E(n_1, n_2) - \sum_k Q_k V_k, \quad (8)$$

where the summation is over the voltage-applied electrodes of the system (four such electrodes in Fig. 1), and Q_k and V_k are the charge and voltage of each such electrode, respectively.

Let us now discuss the crossover behavior of the coupled SET's in detail. For simplicity, let us set $V_2 = 0$ and $V = V_1$ throughout this paper. Nonzero V_2 's do not alter the result here and will be discussed later. Let us restrict ourselves for the moment to the case where the gate voltages are swept such that $q = q_1 = -q_2$. Other gate sweeps will be discussed later. Then, as mentioned above, the crossover region has two charge configurations $(0, 0)$ and $(-1, 1)$. For low V 's, namely, for $V < V_s$ where

$$V_s = \frac{1}{6} \frac{C_\alpha}{C_\alpha + 1}, \quad (9)$$

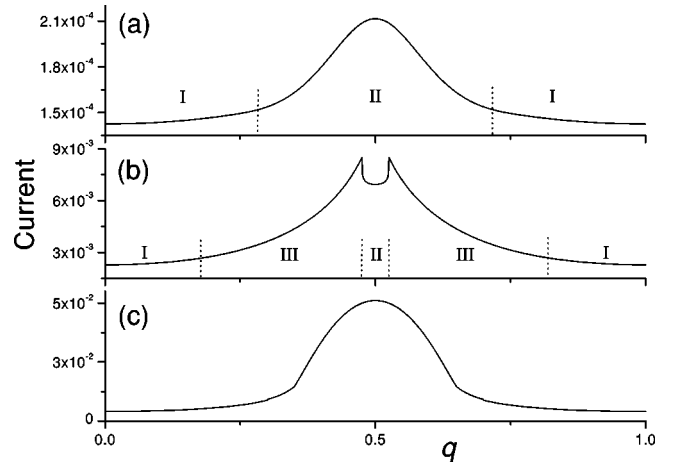


FIG. 3. The current I_1 through the lower SET for the cases of (a) $V < V_s$, (b) V near V_c ($V_s < V < V_c$), and (c) $V > V_c$, for $C_\alpha = 5$; $R = 1 \times 10^5 \Omega$, and temperature $T = 0$. The unit of current is $\tilde{I} \equiv e/R\tilde{C}$. In (a) and (b), the regions for states I, II, and III are marked.

only the tunneling processes of $(0,0) \rightarrow (-1,1) \rightarrow (0,0)$ are possible: that is, only by the second-order cotunneling of simultaneous transfer of an electron and a hole on islands 1 and 2, respectively, can the state $(-1, 1)$ be accessed from the state $(0, 0)$, and vice versa. How we obtained V_s in Eq. (9) will be clarified shortly. On the other hand, for higher V 's, namely, for $V > V_c$ where

$$V_c = \frac{1}{4} \frac{C_\alpha}{C_\alpha + 1}, \quad (10)$$

the dominant tunneling processes are sequential ones: that is, state $(-1, 1)$ is accessed by the sequential tunneling of $(0,0) \rightarrow (-1,0)$ followed by the sequential tunneling of $(-1,0) \rightarrow (-1,1)$ (hole attraction). How we obtained V_c in Eq. (10) will be also clarified shortly. Although a quantum tunneling of the second order still takes place, the cotunneling rate in this case is much smaller than the sequential tunneling rate. In Fig. 3 we show the typical I - q characteristics for the cases of $V < V_s$ [Fig. 3(a)] and $V > V_c$ [Fig. 3(c)].

For intermediate bias voltages of $V_s < V < V_c$, the crossover from the cotunneling-only state to the predominantly sequential-tunneling state takes place. Recall that for $V < V_s$ there are two possible states for the system: the stationary state $(0,0)$ or $(-1,1)$, which we define as state I, and the cotunneling-only state where only the second-order cotunneling $[(0,0) \rightleftharpoons (-1,1)]$ occurs (state II); see Fig. 3(a). As V is increased from V_s , a state starts to appear at the boundaries between states I and II. In this state, or state III, the configuration $(-1,1)$ is accessed from the configuration $(0,0)$ *only* by the second-order cotunneling, as in the case of state II. However from configuration $(-1,1)$, the sequential tunneling processes of $(-1,1) \rightarrow (0,1) \rightarrow (-1,1)$ take place in parallel with the cotunneling processes of $(-1,1) \rightarrow (0,0) \rightarrow (-1,1)$. See Table I for a summary of the aforementioned tunneling processes in different states. As V is further increased from V_s , the region for state III expands, while that for state II shrinks [see Fig. 3(b) for an example]. In fact, the interval \mathcal{R}_{II} of state II with respect to q (for $q = q_1 = -q_2$) is given by

TABLE I. The tunneling processes for the various voltage regions. Note that for $V_s < V < V_c$ two states II and III coexist. The diagonal arrows represent the second-order cotunneling, and others sequential tunneling.

$V < V_s$	$V_s < V < V_c$	$V > V_c$
$(0,0)$ \swarrow $(-1,1)$ State II	$(0,0)$ \swarrow $(-1,1)$ State II	$(0,0)$ $(0,1)$ \swarrow \swarrow $(-1,0)$ $(-1,1)$
	$(0,0)$ $(0,1)$ \swarrow \uparrow $(-1,1)$ State III	$(-1,0) \rightarrow (-1,1)$

$$\mathcal{R}_{\text{II}} = \left[\frac{1}{2} - \xi, \frac{1}{2} + \xi \right], \quad (11)$$

where

$$\xi = \frac{C_\alpha}{4} - (C_\alpha + 1)V, \quad (12)$$

while the interval \mathcal{R}_{III} of state III is (for the left part)

$$\mathcal{R}_{\text{III}} = \left[\frac{1}{2} - \frac{1}{2}(C_\alpha + 1)V, \frac{1}{2} - \xi \right]. \quad (13)$$

From the above relationships, we can see that, at $V = V_c$, the interval \mathcal{R}_{II} reduces to zero and state II disappears. To summarize, we find that the crossover is characterized by the appearance of state III at the start up ($V = V_s$), the coexistence of states II and III in its course, and the termination of state II at the end of the crossover ($V = V_c$). Therefore, V_s is the critical voltage for the appearance of the sequential process $(-1,1) \rightarrow (0,1)$ and V_c for the appearance of the sequential process $(0,0) \rightarrow (-1,0)$. That is, V_s in Eq. (9) was obtained by considering $\Delta F = F(0,1) - F(-1,1) = 0$, and V_c in Eq. (10) by considering $\Delta F = F(-1,0) - F(0,0) = 0$, where the free energy $F(n_1, n_2)$ is given by Eq. (8).

The current dip around the peak is seen when V is near V_c ($V < V_c$); see Fig. 3(b). The appearance of the current dip is due to coexistence and competition of states II and III during the crossover: in the crossover voltage range of $V_s < V < V_c$, the current I through the lower SET (recall that $V_2 = 0$ so that the current through the upper SET is zero) is the sum of the current I_{cot} and the current I_{seq} , where I_{cot} is the current by the cotunneling processes $[(0,0) \rightleftharpoons (-1,1)]$ and I_{seq} is the current by the sequential tunneling processes $[(-1,1) \rightarrow (0,1) \rightarrow (-1,1)]$. Then the current in the region of state II is simply

$$I = I_{\text{cot}}, \quad (14)$$

whereas the current in the region of state III is given by

$$I = I_{\text{cot}} + I_{\text{seq}}. \quad (15)$$

(Note that there is another kind of the cotunneling process, namely, the second-order cotunneling from the source to the drain of the lower SET. However, it simply adds up to the total current as the background current, so we do not include it in the discussion here.) We have found that I_{seq} is negligibly small compared to I_{cot} if V is close to V_s . But as V is increased from V_s , $I_{\text{seq}}/I_{\text{cot}}$ gradually increases, and, when V is close to V_c , I_{seq} becomes comparable to I_{cot} . See Fig. 4, where I_{seq} , I_{cot} , and I are plotted together. We can see from Fig. 4 that I_{cot} simply shows a peak around $q = 1/2$, but I_{seq} shows a behavior where it initially increases with q but sharply drops to zero near the boundaries of states II and III. Recall that in state III, no such sequential tunneling is allowed. When two contributions I_{cot} and I_{seq} are added up, the resultant total current I shows a dip, as shown in the figure. Therefore, we conclude that the appearance of the current dip in the parallel coupled SET's is due to their unique crossover behavior of coexistence and competition of two states with subtly different tunneling mechanisms.

In Fig. 4, the cotunneling rates were calculated using the Jensen-Martinis approximation⁶ to elucidate the sequential tunneling contribution. However, I_{cot} in state II can be calculated via the exact second-order cotunneling formula⁷

$$\Gamma = \frac{R_K}{4\pi^2 e^2 R_1 R_2} \left\{ 2 - \left(1 + \frac{2}{\Delta F} \frac{\Delta F_1 \Delta F_2}{\Delta F - \Delta F_1 - \Delta F_2} \right) \times \left(\sum_{i=1,2} \ln(1 - \Delta F / \Delta F_i) \right) \right\} \Delta F, \quad (16)$$

where ΔF_1 and ΔF_2 are the free energy changes for the intermediate tunneling processes which are involved in the cotunneling process, and ΔF is that for the cotunneling. Then

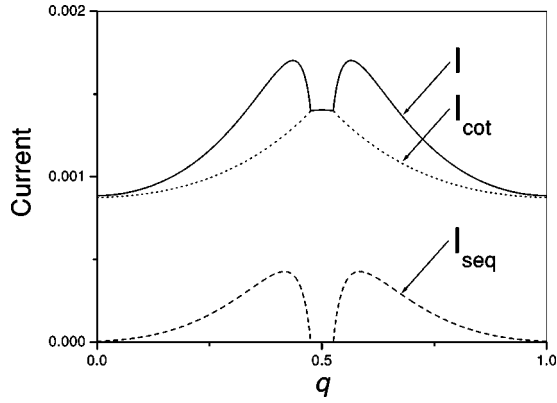


FIG. 4. Contributions of sequential tunneling (I_{seq}) and cotunneling (I_{cot}) to the total current (I) at a V near V_c . $C_\alpha=5$, $R=2 \times 10^5$, and $T=0$, and the Jensen-Martinis approximation was used.

$$I_{\text{cot}} = \frac{\Gamma_{AB}\Gamma_{BA}}{\Gamma_{AB} + \Gamma_{BA}}, \quad (17)$$

where Γ_{AB} is the cotunneling rate for the process $(0,0) \rightarrow (-1,1)$ and Γ_{BA} for the reverse process. In the above equation, $R_K = h/e^2 \approx 25.8 \text{ K}\Omega$, and R_1 and R_2 are the resistances of the junctions involved in the cotunneling process. ΔF_1 and ΔF_2 of the cotunneling process $[(0,0) \rightleftharpoons (-1,1)]$ are $\Delta F_1 = F(-1,0) - F(0,0)$ and $\Delta F_2 = F(-1,1) - F(-1,0)$ where the free energy $F(n_1, n_2)$ is given by Eq. (8). The currents in the regions of states I and II in Fig. 3 were obtained by using the exact formula for the cotunneling rate. However, due to the coexistence of the cotunneling and the sequential tunneling processes in the region of state III, the cotunneling rates were regularized in a standard way for the region. We have also tried another approximation for the cotunneling rate, namely that of Lafarge and Esteve,⁸ and obtained the similar results.

In Fig. 5 we indicate, in a stability diagram, the region of state II where the current dip is observable. The region forms a narrow band in the plane of q_1 and q_2 ; therefore, depending on the way the gate sweep is performed, one has a slightly different width (with respect to the sweep gate voltage) for the current dip. For example, one may fix the upper gate voltage at $q_2 = -1/2$ and sweep over q_1 . The resulting I - q_1 characteristics show a similar current dip but with its width a bit shorter than by the sweep where $q_1 = -q_2$.

We have found that the current dip is best observed for the coupling $1 \lesssim C_\alpha/\bar{C} \lesssim 5$. If the coupling is too weak, the current dip is not so pronounced as to be discerned. On the other

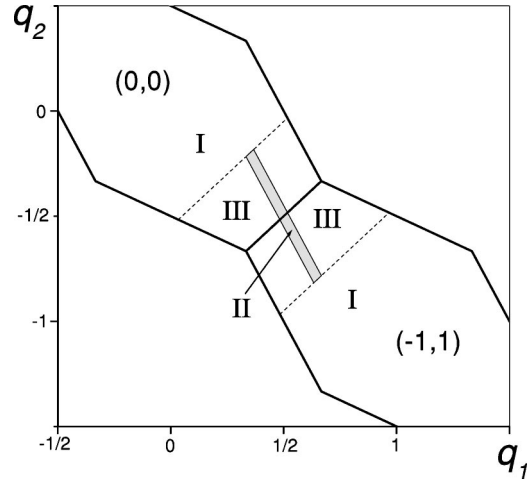


FIG. 5. The honeycombs $(0,0)$ and $(-1,1)$ of the parallel coupled SET's for V near V_c ($V_s < V < V_c$). The shaded region represents the region where the current dip can be observed (state II). The regions for states I and II are also marked.

hand, if the coupling is too strong, the width for the current-dip is too narrow to be observed.

In this study, V_2 of the upper SET has been set to zero for simplicity. For nonzero V_2 , we obtain a similar crossover behavior with the appearance of a current dip near some critical voltage, but the tunneling processes involved are much more complicated than for the case $V_2 = 0$.

As the temperature is increased, the sequential tunneling processes begin to occur in the cotunneling-only region and the current dip becomes shallower. At higher temperatures, then, the whole region can be effectively described by the sequential tunneling processes only. As the result, the current dip is replaced by the usual current peak around $q = 1/2$. The critical temperature for the disappearance of the dip is $T_c/\bar{T} \sim 10^{-3}$, where $\bar{T} \equiv e^2/k_B\bar{C}$. For the tunnel-junction capacitance of the order of 1 aF, T_c is about 1 K.

In conclusion, we have found that parallel coupled single-electron transistors undergo a unique crossover from the cotunneling-only regime to the sequential-tunneling dominant regime. In the course of crossover, two states with subtly different tunneling mechanisms coexist and compete with each other, resulting in a current dip with respect to a gate voltage sweep.

This work was supported by Grant No. 1999-1-11400-002-5 from the Basic Research Program of the Korea Science and Engineering Foundation.

*Email address: mcshin@icu.ac.kr

¹D. V. Averin, A. N. Korotkov, and Yu. V. Nazarov, Phys. Rev. Lett. **66**, 2818 (1991).

²M. Matters, J. J. Versluys, and J. E. Mooij, Phys. Rev. Lett. **78**, 2469 (1997).

³P. Delsing, D. B. Haviland, and P. Davidsson, Czech. J. Phys. **46**, 2359 (1996).

⁴M. Shin, S. Lee, K. W. Park, and G.-H. Kim, Phys. Rev. B **62**, 9951 (2000).

⁵V. A. Krupenin, S. V. Lotkhov, H. Scherer, Th. Weimann, A. B. Zorin, F.-J. Ahlers, J. Niemeyer, and H. Wolf, Phys. Rev. B **59**, 10 778 (1999).

⁶H. D. Jensen and J. M. Martinis, Phys. Rev. B **46**, 13407 (1992).

⁷D. V. Averin and Yu. V. Nazarov, in *Single Charge Tunneling*, edited by H. Grabert and M. H. Devoret (Plenum, New York, 1991), p. 217, and references therein.

⁸P. Lafarge and D. Esteve, Phys. Rev. B **48**, 14 309 (1993).